Seismic resolution and illumination: A wave-equation-based analysis

*Xiao-Bi Xie*and Ru-Shan Wu, IGPP, University of California, Santa Cruz,*
Michael Fehler and Lianjie Huang, Los Alamos National Laboratory

SUMMARY

We develop a method to evaluate the resolution of seismic images using a wave-equation-based operator. The one-way wave-equation-based propagator is used to extrapolate the wavefields from both the source and receivers to a target region. The plane wave analysis method is used to decompose the wavefields and calculate the wavenumber domain resolution function. The method can be applied to complex models without smoothing velocity. It can also handle irregular acquisition geometry and finite frequency band. The resulting resolution function can be used to estimate image quality or correct the image distortion caused by the uneven illumination.

INTRODUCTION

The effect of acquisition on resolution of a seismic image can be evaluated using the coverage of scattering wavenumbers in the target Fourier space (Beylkin, et al., 1985). This coverage is affected by the acquisition configuration, the background velocity model and the frequency band of the signal. Due to the irregular acquisition geometry and complex velocity model involved in the seismic migration imaging processes, the resolution analysis is usually conducted using simplified model geometries or using the ray-based high-frequency asymptotic methods (e.g., Schuster and Hu, 2000; Gibson and Tzimeas, 2002; Yu and Schuster, 2003). The seismic illumination analysis shares many common basis with the resolution analysis (Muerdter and Ratcliff, 2001ab; Muerdter et al., 2001; Berkhout et al., 2001; and Volker et al., 2001). However, traditionally illumination analysis mostly focuses on how the model space is covered by seismic energy and there is no emphasis on image distortion caused by illumination.

Recently, progresses have been made in several related areas. The angle related information is emphasized in the illumination analysis and the relationship between the illumination and resolution being investigated (Gelius, et al., 2002; Lecomte, et al. 2003). The local angle related information has been extracted from the wave-equation-based propagators and applied to the illumination analysis (Xie and Wu, 2002; Wu and Chen, 2002, 2003; Wu et al. 2003; Xie et al. 2003, 2004).

In this paper, we investigate the relationship between the resolution and illumination using the wave-equation-based propagator. The resolution function can be calculated in both wavenumber and space domains. The new method has the advantage of handling wave motion phenomena. The complex models can be treated without smoothing velocity. Finite frequency band can be used in the calculation. This method can also handle irregular acquisition geometries. To demonstrate potential applications of this method, numerical examples are calculated using the 2D SEG/EAGE salt model.

This analysis neglects the influence of different approximations of migration operators and variations of the model from the true structure to the resolution. For a full theory of imaging resolution including the influence of imperfect propagators, and the related numerical examples, see our other studies (Wu, et al., 2005; Fehler, et al., 2005).

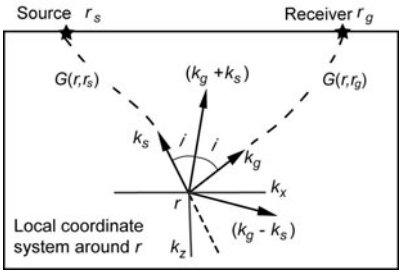

Figure 1. Coordinate system used in the analysis.

FORMULATION

Consider using a survey system composed of a source located at $\mathbf{r}_s$ and a receiver located at $\mathbf{r}_g$ to investigate the subsurface target within a small region $V(\mathbf{r})$ neighboring location $\mathbf{r}$ (see Figure 1). With one-way Green's functions for heterogeneous background velocity model, the reflection seismic data can be expressed as

$$u(\mathbf{r},\mathbf{r}_s,\mathbf{r}_g) = 2k_0^2 \int_V m(\mathbf{r}') G(\mathbf{r}';\mathbf{r}_s) G(\mathbf{r}';\mathbf{r}_g)\, dv', \qquad (1)$$

where $m(\mathbf{r}) = \delta c/c(\mathbf{r}')$ is the velocity perturbation, $k_0 = \omega/c_0(\mathbf{r})$ is the background wavenumber and c_0 is a local background velocity. Equation (1) and the following equations are in frequency domain but we omit the apparent frequency variable. The prestack depth image I at location $\mathbf{r}''$ within V can be expressed as

$$\begin{aligned} I(\mathbf{r},\mathbf{r}'',\mathbf{r}_s,\mathbf{r}_g) &= G^*(\mathbf{r}'';\mathbf{r}_s) G^*(\mathbf{r}'';\mathbf{r}_g) u(\mathbf{r},\mathbf{r}_s,\mathbf{r}_g) \\ &= 2k_0^2 G^*(\mathbf{r}'';\mathbf{r}_s) G^*(\mathbf{r}'';\mathbf{r}_g) \int_V m(\mathbf{r}') G(\mathbf{r}';\mathbf{r}_s) G(\mathbf{r}';\mathbf{r}_g)\, dv'. \end{aligned} \qquad (2)$$

The Green's functions G in above equations can be decomposed into plane waves within V

$$G(\mathbf{r}';\mathbf{r}_{s,g}) = \int G(\mathbf{k},\mathbf{r};\mathbf{r}_{s,g}) e^{i\mathbf{k}\cdot\mathbf{r}'} d\mathbf{k}. \qquad (3)$$

Substituting equation (3) into equation (2), we obtain

$$\begin{aligned} &I(\mathbf{r},\mathbf{r}'',\mathbf{r}_s,\mathbf{r}_g) = \\ &= \iint A(\mathbf{r},\mathbf{k}_s,\mathbf{k}_g;\mathbf{r}_s,\mathbf{r}_g) m(\mathbf{r},\mathbf{k}_s+\mathbf{k}_g) e^{i(\mathbf{k}_s+\mathbf{k}_g)\mathbf{r}''} d\mathbf{k}_s d\mathbf{k}_g, \end{aligned} \qquad (4)$$

Seismic resolution and illumination

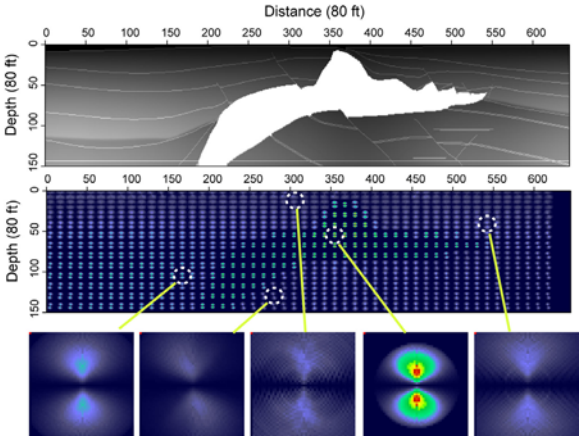

Figure 2. Upper panel: 2-D SEG/EAGE salt velocity model; Middle panel: Wavenumber domain resolution functions; and Bottom panel: Enlarged resolution functions for selected locations.

where

$$m(\mathbf{r},\mathbf{k}_s+\mathbf{k}_g)=\int_V m(\mathbf{r}')e^{i(\mathbf{k}_s+\mathbf{k}_g)\cdot\mathbf{r}'}dv', \tag{5}$$

$$A(\mathbf{r},\mathbf{k}_s,\mathbf{k}_g;\mathbf{r}_s,\mathbf{r}_g)=2k_0^2G^*(\mathbf{k}_s,\mathbf{r};\mathbf{r}_s)G(\mathbf{k}_s,\mathbf{r};\mathbf{r}_s)\times G^*(\mathbf{k}_g,\mathbf{r};\mathbf{r}_g)G(\mathbf{k}_g,\mathbf{r};\mathbf{r}_g). \tag{6}$$

In above equations, $\mathbf{k}_s$ and $\mathbf{k}_g$ are local transforms with respect to $\mathbf{r}'$ or $\mathbf{r}''$ (not $\mathbf{r}_s$ and $\mathbf{r}_g$), subscripts *s* and *g* are for source- and receiver-side wavefields, respectively. In equation (4), introducing transforms $\mathbf{k}_d=\mathbf{k}_g+\mathbf{k}_s$ and $\mathbf{k}_c=\mathbf{k}_g-\mathbf{k}_s$, integrating $A(\mathbf{r},\mathbf{k}_d,\mathbf{k}_c,\mathbf{r}_s,\mathbf{r}_g)$ with respect to $\mathbf{k}_c$ and recovering the frequency variable ω, we have

$$I(\omega,\mathbf{r},\mathbf{r}'',\mathbf{r}_s,\mathbf{r}_g)=s(\omega)\int A(\omega,\mathbf{r},\mathbf{k}_d;\mathbf{r}_s,\mathbf{r}_g)m(\mathbf{r},\mathbf{k}_d)e^{i\mathbf{k}_d\cdot\mathbf{r}''}d\mathbf{k}_d, \tag{7}$$

where $s(\omega)$ is the source spectrum, $A(\omega,\mathbf{r},\mathbf{k}_d,\mathbf{r}_s,\mathbf{r}_g)$ is the wavenumber domain illumination function given by Xie, et al. (2004). For an acquisition system composed of multiple sources and receivers and within a finite frequency band, the image can be expressed as

$$I(\mathbf{r},\mathbf{k}_d)=R(\mathbf{r},\mathbf{k}_d)m(\mathbf{r},\mathbf{k}_d), \tag{8}$$

where

$$R(\mathbf{r},\mathbf{k}_d)=\int s(\omega)\sum_{\mathbf{r}_s}\sum_{\mathbf{r}_g}A(\omega,\mathbf{r},\mathbf{k}_d,\mathbf{r}_s,\mathbf{r}_g)d\omega. \tag{9}$$

Equation (8) can be expressed in the space domain as well

$$I(\mathbf{r},\mathbf{r}'')=R(\mathbf{r},\mathbf{r}'')*m(\mathbf{r},\mathbf{r}''), \tag{10}$$

where "$*$" stands for the convolution with respect to $\mathbf{r}''$ and

$$R(\mathbf{r},\mathbf{r}'')=\int R(\mathbf{r},\mathbf{k}_d)e^{i\mathbf{k}_d\cdot\mathbf{r}''}d\mathbf{k}_d \tag{11}$$

Equations (9) and (11) give the point spreading function in wavenumber and space domains. They are related by the Fourier transform. Equation (9) also shows the relationship between the illumination and resolution. We see from equations (8) and (10) that the image I is a distorted version of the model m. These equations show that, given the resolution function R, one can generate a synthetic "migration image" by convolving R with the model m (Lecomte, et al. 2003), or correct the illumination caused image distortion by deconvolving R from the migration images (Sjoeberg and Lecomte, 2003).

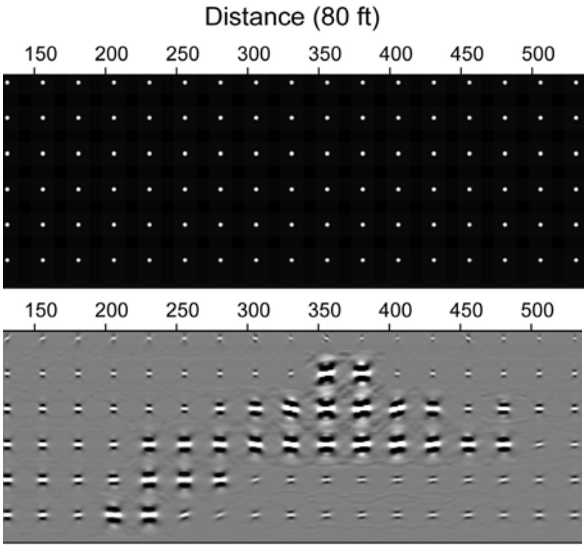

Figure 3. Upper panel: Point scatters used to test the resolution function. Lower panel: Point spreading functions in the SEG/EAGE salt model. The center frequency of the Ricker wavelet is 15 Hz.

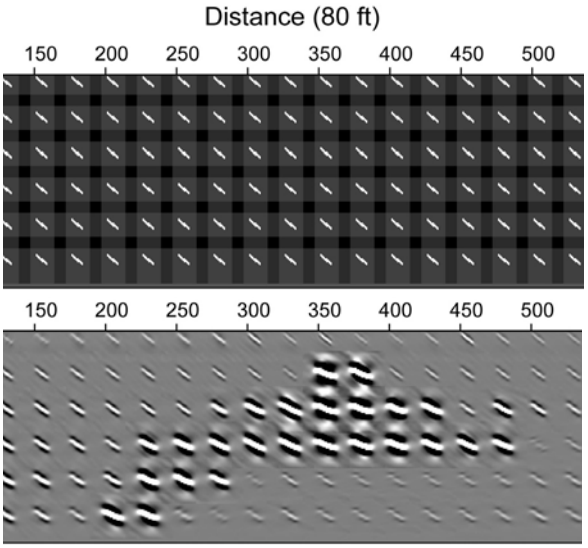

Figure 4. Upper panel: Small 40-degree dipping structures used to test the resolution function. Lower panel: The migration images of the dipping structures in the SEG/EAGE salt model. The center frequency of the Ricker wavelet is 15 Hz.

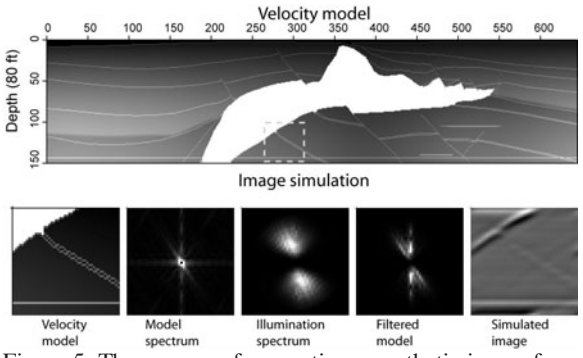

Figure 5. The process of generating a synthetic image from the velocity model. Shown in the upper panel is velocity model, and in the lower panel are localized operations from velocity model to synthetic image. The dashed square indicates the region under processing.

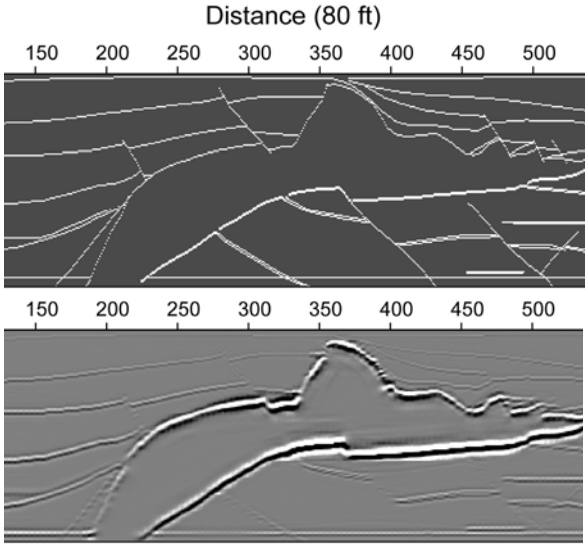

Figure 6. Upper panel: Reflectors in the SEG/EAGE salt velocity model. Lower panel: Synthetic prestack depth image.

NUMERICAL EXAMPLES

To demonstrate the resolution analysis using a wave-equation propagator, a group of numerical examples are calculated using the 2-D SEG/EAGE salt model and its acquisition configuration. The wavefield is extrapolated using a wide-angle one-way propagator (Xie and Wu, 1998). Shown in Figure 2 are the velocity model and the wavenumber domain resolution function using equation (9). The enlarged resolution functions are shown for selected locations in the bottom panel of Figure 2. In the sub-salt region, the resolution function is weak and distorted, resulting in poor-quality images for structures oriented in certain directions.

Two examples are calculated to show the responses of structures to the background velocity model and acquisition system. The upper panel of Figure 3 shows an array of point scatters embedded in the SEG/EAGE salt model. The resulting images in the lower panel of Figure 3 simulate the point spreading functions at different locations in the model. In Figure 4, an array of 40-degree dipping reflectors is used. The migration image reveals the illumination to the specific dipping angle.

Figure 5 explains the process of generating a synthetic image. The upper panel is the velocity model. The region within the dashed square is chosen to demonstrate the precess. In the lower panel and from left to right, the velocity model is Fourier transformed to the wavenumber domain and filtered by the wavenumber domain resolution function. Then, the filtered model is transformed back to the space domain. Repeating this process for the entire model generates the synthetic image. Shown in Figure 6 are the reflectors and synthetic image generated using this technique.

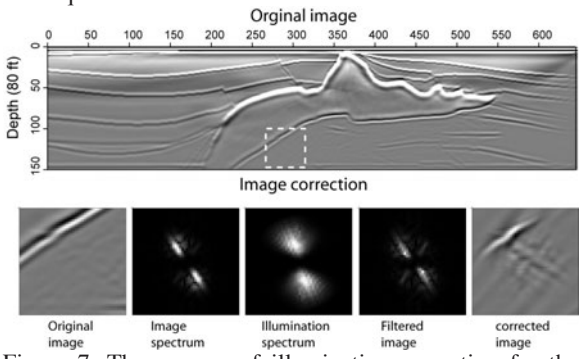

Figure 7. The process of illumination correction for the prestack depth image. Upper panel: Prestack image of the salt model; Lower panel: localized operations for image correction. The dashed square indicates the region under processing.

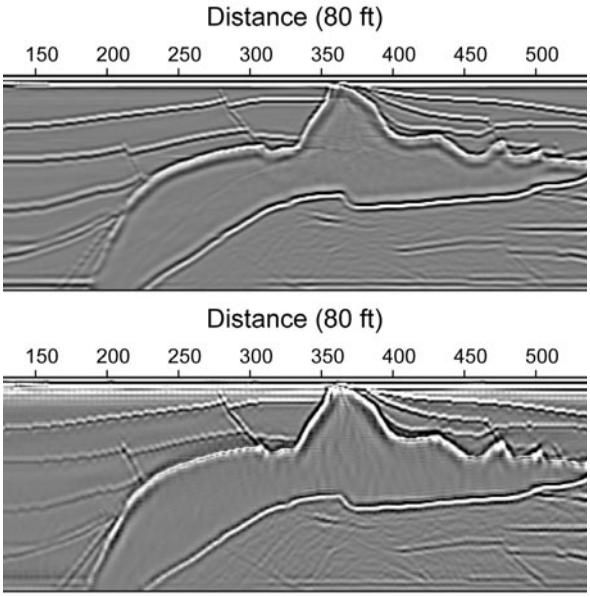

Figure 8. Upper panel: The original prestack depth image for the salt model. Lower panel: Resolution deconvolved depth image.

Figure 7 explains the process of image correction. The upper panel is the prestack depth image. The region within the dashed square is chosen to demonstrate the processing. In the Lower panel and from left to right, the depth image is Fourier transformed to the wavenumber domain and the resolution function is deconvolved from the image. The process is actually conducted in the wavenumber domain by division. Proper water level is used to maintain the stability. The modified spectrum is transformed back to the space domain and forms the modified image. Repeating this process for the entire model generates the resolution deconvolved image. Figure 8 shows the original depth image and the resolution deconvolved image. The images of the subsalt structures, particularly some of the steeply dipping structures, are improved.

CONCLUSIONS

In this research, we developed a method for resolution and illumination analysis. Using the wave-equation-based propagator and plane wave decomposition, the method can be applied to complex models without smoothing velocity. Different acquisition configurations can be adopted in the calculation. The resolution function can be used to simulate a synthetic migration image, correct the depth image, and conduct illumination analysis for specific acquisition systems and velocity models.

Acknowledgement. The research is supported by the DOE/BES Project jointly conducted at the University of California, Santa Cruz and Los Alamos National Laboratory.

REFERENCES

Beylkin G., Oristaglio M. and Miller D. 1985, Spatial resolution of migration algorithms, in Proceedings of the 14th International Symposium on Acoustic Imaging, pp. 155-167. Plenum Press.

Berkhout, A. J., Ongkiehongz, L., Volker, A. W. F., and Blacquière, G., 2001, Comprehensive assessment of seismic acquisition geometries by focal beams—Part I: Theoretical considerations, Geophysics, 66, 911-917.

Fehler, M., Huang, L., Wu, R.S., and Xie, X.B., 2005, Seismic image resolution: Numerical investigation of role of migration imaging operator, 75th Annual International Meeting, SEG, Expanded Abstracts, submitted.

Gelius, L.J., Lecomte, I., and Tabti, H., 2002, Analysis of the resolution function in seismic prestack depth imaging, Geophysical Prospecting, 50, 505-515.

Gibson, R.L. and Tzimeas, C., 2002, Quantitative measures of image resolution for seismic survey design, Geophysics, 67, 1844-1852.

Lecomte, I., Gjoystdal, I.H., and Drottning, A., 2003, Simulated Prestack Local Imaging: a robust and efficient interpretation tool to control illumination, resolution, and time-lapse properties of reservoirs, 73rd Annual International Meeting, SEG, Expanded Abstracts, 1525-1528.

Muerdter, D., Kelly, M. and Ratcliff, D., 2001, Understanding subsalt illumination through ray-trace modeling, Part 2: Dipping salt bodies, salt peaks, and nonreciprocity of subsalt amplitude response, The Leading Edge, **20**, 688-697.

Muerdter, D. and Ratcliff, D., 2001a, Understanding subsalt illumination through ray-trace modeling, Part 1: Simple 2-D salt models, The Leading Edge, **20**, 578-594.

Muerdter, D. and Ratcliff, D., 2001b, Understanding subsalt illumination through ray-trace modeling, Part 3: Salt ridges and furrows, and the impact of acquisition orientation, The Leading Edge, **20**, 803-816.

Schuster, G.T., and Hu, J., 2000, Green's function for migration: Continuous recording geometry, Geophysics, 65, 167-175.

Sjoeberg, T.A. and Lecomte, I., 2003, 2-D deconvolution of seismic image blur, 73rd Annual International Meeting, SEG, Expanded Abstracts, 1055-1058.

Volker, A. W. F., Blacquière, G., Berkhout, A. J., and Ongkiehong, L., 2001, Comprehensive assessment of seismic acquisition geometries by focal beams—Part II: Practical aspects and examples, Geophysics, 66, 918-931.

Wu, R.S. and Chen, L, 2002, Mapping directional illumination and acquisition-aperture efficacy by beamlet propagators: 72nd Annual International Meeting, SEG, Expanded Abstracts, 1352-1355.

Wu, R.S., and Chen, L., 2003, Prestack depth migration in angle-domain using beamlet decomposition: Local image matrix and local AVA, 73rd Annual International Meeting, SEG, Expanded Abstracts, 973-976.

Wu, R.S., Chen, L., and Xie, X.B., 2003, Directional illumination and acquisition dip-response, 65th Conference and Technical Exhibition, EAGE, Expanded abstracts, P147.

Wu, R.S. et al., 2005, Spatial resolution of seismic imaging, 75th Annual International Meeting, SEG, Expanded Abstracts, submitted.

Xie, X.B., Jin, S., and Wu, R.S., 2003, Three-dimensional illumination analysis using wave equation based propagator: 73rd Annual International Meeting, SEG, Expanded Abstracts, 989-992.

Xie, X.B., S. Jin, and R.S. Wu, 2004, Wave equation based illumination analysis: 74th Annual International Meeting, SEG, Expanded Abstracts, 933-936.

Xie, X.B., and Wu, R.S., 1998, Improve the wide-angle accuracy of screen method under large contrast: 68th Annual International Meeting, SEG, Expanded Abstracts, 1247-1250.

Xie, X.B. and Wu, R.S., 2002, Extracting angle domain information from migrated wavefield: 72nd Annual International Meeting, SEG, Expanded Abstracts, 1360-1363.

Yu, J., and Schuster, G.T., 2003, 3-D prestack migration decomvolution: 73rd Annual International Meeting, SEG, Expanded Abstracts, 1651-1654.

EDITED REFERENCES

Note: This reference list is a copy-edited version of the reference list submitted by the author. Reference lists for the 2005 SEG Technical Program Expanded Abstracts have been copy edited so that references provided with the online metadata for each paper will achieve a high degree of linking to cited sources that appear on the Web.

Seismic resolution and illumination: A wave-equation-based analysis
References

Beylkin, G., M. Oristaglio, and D. Miller, 1985, Spatial resolution of migration algorithms: Plenum Press, 155–167.

Berkhout, A. J., L. Ongkiehongz, A. W. F. Volker, and G. Blacquière, 2001, Comprehensive assessment of seismic acquisition geometries by focal beams—Part I: Theoretical considerations: Geophysics, **66**, 911–917.

Fehler, M., L. Huang, R. S. Wu, and X. B. Xie, 2005, Seismic image resolution: Numerical investigation of role of migration imaging operator: Presented at the 75th Annual International Meeting, SEG.

Gelius, L. J., I. Lecomte, and H. Tabti, 2002, Analysis of the resolution function in seismic prestack depth imaging: Geophysical Prospecting, **50**, 505–515.

Gibson, R. L., and C. Tzimeas, 2002, Quantitative measures of image resolution for seismic survey design: Geophysics, **67**, 1844–1852.

Lecomte, I., I. H. Gjoystdal, and A. Drottning, 2003, Simulated prestack local imaging: A robust and efficient interpretation tool to control illumination, resolution, and time-lapse properties of reservoirs: 73rd Annual International Meeting, SEG, Expanded Abstracts, 1525–1528.

Muerdter, D., M. Kelly, and D. Ratcliff, 2001, Understanding subsalt illumination through ray-trace modeling, Part 2: Dipping salt bodies, salt peaks, and nonreciprocity of subsalt amplitude response: The Leading Edge, **20**, 688–697.

Muerdter, D., and D. Ratcliff, 2001a, Understanding subsalt illumination through ray-trace modeling, Part 1: Simple 2-D salt models: The Leading Edge, **20**, 578–594.

—, 2001b, Understanding subsalt illumination through ray-trace modeling, Part 3: Salt ridges and furrows, and the impact of acquisition orientation: The Leading Edge, **20**, 803–816.

Schuster, G. T., and J. Hu, 2000, Green's function for migration: Continuous recording geometry: Geophysics, **65**, 167–175.

Sjoeberg, T. A., and I. Lecomte, 2003, 2-D deconvolution of seismic image blur: 73rd Annual International Meeting, SEG, Expanded Abstracts, 1055–1058.

Volker, A. W. F., G. Blacquière, A. J. Berkhout, and L. Ongkiehong, 2001, Comprehensive assessment of seismic acquisition geometries by focal beams—Part II: Practical aspects and examples: Geophysics, **66**, 918–931.

Wu, R. S., 2005, Spatial resolution of seismic imaging: Pesented at the 75th Annual International Meeting, SEG.

Wu, R. S., and L. Chen, 2002, Mapping directional illumination and acquisition-aperture efficacy by beamlet propagators: 72nd Annual International Meeting, SEG, Expanded Abstracts, 1352–1355.

—, 2003, Prestack depth migration in angle-domain using beamlet decomposition: Local image matrix and local AVA: 73rd Annual International Meeting, SEG, Expanded Abstracts, 973–976.
Wu, R. S., L. Chen, and X. B. Xie, 2003, Directional illumination and acquisition dip-response: 65th Annual International Conference and Exhibition, EAGE, Expanded Abstracts, P147.
Xie, X. B., S. Jin, and R. S. Wu, 2003, Three-dimensional illumination analysis using wave equation based propagator: 73rd Annual International Meeting, SEG, Expanded Abstracts, 989–992.
—, 2004, Wave equation based illumination analysis: 74th Annual International Meeting, SEG, Expanded Abstracts, 933–936.
Xie, X. B., and R. S. Wu, 1998, Improve the wide-angle accuracy of screen method under large contrast: 68th Annual International Meeting, SEG, Expanded Abstracts, 1247–1250.
—, 2002, Extracting angle domain information from migrated wavefield: 72nd Annual International Meeting, SEG, Expanded Abstracts, 1360–1363.
Yu, J., and G. T. Schuster, 2003, 3D prestack migration decomvolution: 73rd Annual International Meeting, SEG, Expanded Abstracts, 1651–1654.